Staging energy sources to extend flight time of a multirotor UAV

Karan P. Jain[1], Jerry Tang[1], Koushil Sreenath[2], and Mark W. Mueller[1]

***Abstract*— Energy sources such as batteries do not decrease in mass after consumption, unlike combustion-based fuels. We present the concept of staging energy sources, i.e. consuming energy in stages and ejecting used stages, to progressively reduce the mass of aerial vehicles in-flight which reduces power consumption, and consequently increases flight time. A flight time vs. energy storage mass analysis is presented to show the endurance benefit for multirotors on staging. We consider two specific problems in discrete staging – optimal order of staging given a certain number of energy sources, and optimal partitioning of a given energy storage mass budget into a given number of stages. We then derive results for two continuously staged cases – an internal combustion engine driving propellers, and a rocket engine. A fundamental flight time limit is seen for the internal combustion engine case, but not for the rocket engine, suggesting that rocket engines could be a better choice in certain scenarios. Lastly, we conduct flight experiments[a] on a custom two-stage battery-powered quadcopter. This quadcopter can eject a battery stage after consumption in-flight using a custom-designed mechanism, and continue hovering using the next stage. The experimental flight times are compared with those predicted from the analysis for our vehicle. The values match well which validates the presented staging analysis.**

I. Introduction

A. Motivation

The ability to fly has given rise to the use of unmanned aerial vehicles (UAVs) in several applications such as surveillance [1], mapping [2], delivery [3], and search and rescue missions [4]. A fundamental limitation of most UAVs is their flight time – they must land when their energy source is depleted. There is a growing demand for higher endurance and range in UAVs with their increasing usage in the research, commercial, and industrial settings.

B. Literature review

Innovative approaches have been explored to increase the flight time of UAVs. Broadly, we can classify the approaches into two types: assisted and unassisted.

Assisted methods typically involve the use of fixed stations or mobile vehicles for the replacement or the charging of energy sources. Battery swapping at a fixed ground station has been presented in [5]–[7], and on a mobile ground base has been shown in [8]. Flying replacement batteries to a multirotor using other multirotors is discussed in [9].

Unassisted methods typically involve increasing mechanical or electrical efficiency or the use of optimization-based methods over objectives such as flight time or range. One such approach is exploiting the efficiency of a fixed-wing and hovering ability of a multirotor by converting them into a hybrid aerial vehicle [10], [11]. Vehicle structure manipulation by tilting rotors to increase efficiency is shown in [12]. An online strategy for optimizing efficiency by altering flight parameters (e.g. speed) over a trajectory is presented in [13]. The usage and analysis of a solar-powered UAV, which can potentially fly for a really long time, are discussed in [14]. However, such a vehicle requires a large wing-span, is sensitive to weather conditions, and is not suitable for indoor settings.

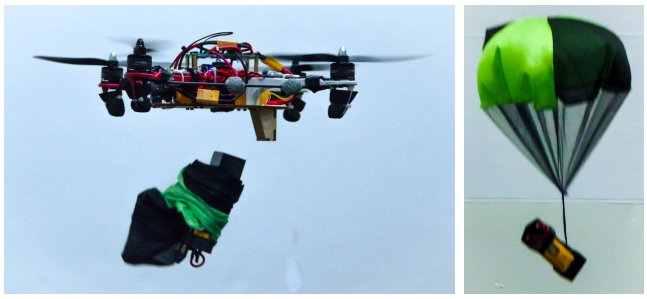

Fig. 1. (Left:) Quadcopter dropping its first stage after use. A parachute is attached to the ejected stage to avoid damage to the battery or the surroundings. (Right:) Ejected stage with the deployed parachute.

An unassisted approach which is largely unexplored for UAVs is the staging of energy sources. A possibility of ejecting depleted energy sources is mentioned in [15], which presents a modular drone consisting of drone cells, which can potentially be staged. Energy sources such as batteries are used widely on UAVs, primarily because they are easy to recharge and reuse, and are non-polluting, making them a good candidate for indoor settings. Electric powertrains also have fewer moving parts, making maintenance easy. Batteries, however, have a clear disadvantage as opposed to combustion fuels, in the sense that the consumed portion still remains as a mass on the vehicle. This has a significant impact because in the case of electric vehicles, battery mass accounts for a notable fraction of the total mass. We take inspiration from multi-stage rockets [16]–[18] which are designed for missions that would otherwise require a much larger single-stage rocket. Staging reduces the overall mass and reduces the amount of fuel required. We note that rocket staging is about discretely staging the structure, not the fuel.

C. Contributions of this work

In this paper, we explore applications of the energy storage staging concept to multirotors. The specific contributions of

The authors are with the [1]High Performance Robotics Lab and [2]Hybrid Robotics group, Dept. of Mechanical Engineering, UC Berkeley, CA 94720, USA. {karanjain, jerrytang, koushils, mwm}@berkeley.edu

[a]The explanation and experimental validation video can be found here: https://youtu.be/_ZBHVZnr8Gk

this paper with respect to previous work are outlined in the following paragraphs.

In Section II, we present a flight time vs. energy storage mass analysis for multirotor aerial vehicles. We then consider two specific optimal staging design problems for discrete energy storage stages. First, given a certain number of energy source stages of different masses, we prove that the optimal order of using these is from the heaviest first to the lightest last. Second, given an energy source mass budget, we show the optimal way to partition it into a given number of stages to maximize flight time. We also consider the effect on flight time for the case of continuously staged energy sources such as combustion fuels or reaction engines, and conclude that combustion driven propellers have a fundamental limit on flight time that reaction engines do not.

In Section III, we discuss the design of an experimental vehicle (a quadcopter) whose batteries can be staged. Fig. 1 shows the quadcopter ejecting its first stage, and hovering using its second stage.

In Section IV, we predict the flight times from the staging analysis for a single-stage case vs. a two-stage case for our quadcopter. We then experimentally demonstrate that by consuming batteries successively in discrete stages and detaching the used stages, an increase in flight time is observed. The predicted and experimental flight times are compared to validate the staging analysis.

We note that discarding batteries in the open can be costly and dangerous as impact to batteries might set them on fire and damage surroundings. Care must be taken to safely land the ejected stages (e.g. by using a parachute) so that they can be reused, and so they do not become a hazard to society.

II. Staging Analysis

In this section, we present an analysis of how using an energy source in stages is beneficial for the flight time performance of hovering multirotors. A brief review is first given of the actuator disk model for power consumption of a propeller; this model is then applied to quantify the gain in flight time by discarding the used energy storage stages in-flight. This is then compared to two cases where an infinite number of stages exist: first when the energy source is the fuel combusted (and then exhausted) in an engine that drives rotors, and secondly where the rotors themselves are replaced by rocket motors.

A. Rotor power consumption and flight time

For an idealized ("actuator disk") model of a propeller that is not translating in the ambient air, the aerodynamic power p_{aero} required may be computed [19] as

$$p_{\text{aero}} = \frac{f^{\frac{3}{2}}}{\sqrt{2\rho A_p}}, \tag{1}$$

where f is the thrust produced, ρ is the density of the air, and A_p is the area swept by the rotor. This derivation assumes that the flow is inviscid, incompressible, and follows from applying conservation of mass and energy to a control volume containing the propeller. Note that translating propellers have more complex relationships, see e.g. [13].

The actual power drawn from the energy source to the actual system will include additional losses, including aerodynamic losses which may be captured in a propeller's figure of merit [19] as well as losses in transmission of power to the propeller (e.g. gears or electric resistance). We make the simplifying assumption that these losses are all proportional to the power drawn, so that the actual power consumption of a propeller i producing thrust f_i may be captured by

$$p_i = c_p f_i^{\frac{3}{2}}, \tag{2}$$

where the constant c_p is a function of the propeller size, ambient air density, propeller figure of merit, and powertrain efficiency. Note that a similar relationship can be derived from the mechanical power required to drive the propeller shaft under the assumption that the thrust is proportional to the rotational speed of the propeller squared, and that the propeller torque is proportional to the propeller thrust [12].

For a symmetric quadcopter of mass m to hover, each propeller must produce a force equal to a quarter of the vehicle's weight, and the total power consumption p is

$$p = \sum_i p_i = \frac{1}{2} c_p g^{\frac{3}{2}} m^{\frac{3}{2}}. \tag{3}$$

The local acceleration due to gravity is given by g. Let e_b be the specific energy of the energy source, so the energy budget E for a given energy source mass m_E is $E = e_b m_E$. Then, at constant total mass m, a vehicle with energy energy source E can hover for a flight time of

$$T_f = \frac{E}{p} = e_b c_T m_E m^{-\frac{3}{2}}, \tag{4}$$

where $c_T = 2 c_p^{-1} g^{-\frac{3}{2}}$ is a vehicle-specific constant, and is specifically independent of the vehicle mass.

B. Discrete energy storage stages

A primary disadvantage of batteries for energy storage is that the storage mass does not decrease as the chemical energy is depleted (unlike, for example, a combustion engine). From (3), it is clear that the power consumption would be reduced if the total mass of the vehicle could be reduced, for example by ejecting parts of the vehicle's battery as it is depleted. We will assume that all the energy storage stages have equal specific energy (energy per unit mass).

For a vehicle with N battery stages, where the i^{th} battery has mass m_i, the total mass of the vehicle at stage i is given by $m_d + \sum_{j=i}^{N} m_j$, where m_d is the dry mass of the vehicle, i.e. mass of all components of the vehicle excluding energy storage (but including payload, etc.). In particular, at stage i, the mass $\sum_{j=1}^{i-1} m_j$ has been ejected. The flight time for the i^{th} stage can be computed from (4) as

$$T_{f,i} = e_b c_T m_i \left(m_d + \sum_{j=i}^{N} m_j \right)^{-\frac{3}{2}}, \tag{5}$$

with total flight time over all stages

$$T_f = \sum_i T_{f,i} = e_b c_T \sum_{i=1}^{N} m_i \left(m_d + \sum_{j=i}^{N} m_j \right)^{-\frac{3}{2}}. \quad (6)$$

This equation shows that achievable flight time is directly proportional to the specific energy e_b and depends on the stage masses m_i in a nonlinear fashion.

1) Equal staging: For a vehicle with dry mass m_d, and total energy storage mass m_b split equally over N stages, the flight time can be computed from (4) (after some manipulation) as

$$T_f = \frac{e_b\, c_T\, m_b}{N} \sum_{i=1}^{N} \left(m_d + \frac{i}{N} m_b \right)^{-\frac{3}{2}}. \quad (7)$$

Fig. 2 shows plots of (normalized) flight time vs. the ratio of total energy storage mass (m_b) to total initial vehicle mass (m_d+m_b), for a different number of stages. The case of equal staging is plotted using solid curves.

The plots in Fig. 2 and the results from equal staging can be used in the following ways. For a given energy storage mass, one can fix the x-axis value, and decide the number of stages they want based on their flight time requirements. On the other hand, the choice for designers might be flight time for their vehicle. In that case, they can fix the y-axis value, and then choose the number of stages based on the mass constraints.

2) Optimal staging order: We consider the case of having a series of N energy storage stages, of known, fixed but different masses, with the only design variable being the order in which to stage them. We prove that the optimal flight time is achieved by staging in order of decreasing mass, so that the heaviest stage is depleted and discarded first.

The proof follows by contradiction: assume that an optimal staging sequence is given by $\mathcal{S}^* = \{m_1, m_2, \ldots, m_N\}$ where for some value $k \in \{1, \ldots, N\}$ the stage k is lighter than the following stage $k+1$, i.e. $m_k < m_{k+1}$. Let T^* represent the total flight time, computed with (6) for this sequence.

Let $\bar{\mathcal{S}} := \{m_1, \ldots, m_{k-1}, m_{k+1}, m_k, m_{k+2}, \ldots, m_N\}$ represent a modified staging order, which only changes the order of the original kth stage with $(k+1)$th, and let $\bar{T}$ represent the associated total flight time. We note that the first $k-1$ and the stages continuing after $k+2$ are identical. We compare the total flight time. We denote the short-hand $M := m_d + \sum_{i=k+2}^{N} m_i$ as the total mass of the vehicle after discarding both the stages k and $k+1$. Then the difference in flight times is

$$\begin{aligned} \frac{T^* - \bar{T}}{e_b c_T} =& \frac{m_k}{(M + m_k + m_{k+1})^{\frac{3}{2}}} + \frac{m_{k+1}}{(M + m_{k+1})^{\frac{3}{2}}} \\ & - \frac{m_{k+1}}{(M + m_k + m_{k+1})^{\frac{3}{2}}} - \frac{m_k}{(M + m_k)^{\frac{3}{2}}} \quad (8) \\ =& (m_k - m_{k+1})\, q\,(m_k + m_{k+1}) \\ & + m_{k+1} q\,(m_{k+1}) - m_k q\,(m_k), \quad (9) \end{aligned}$$

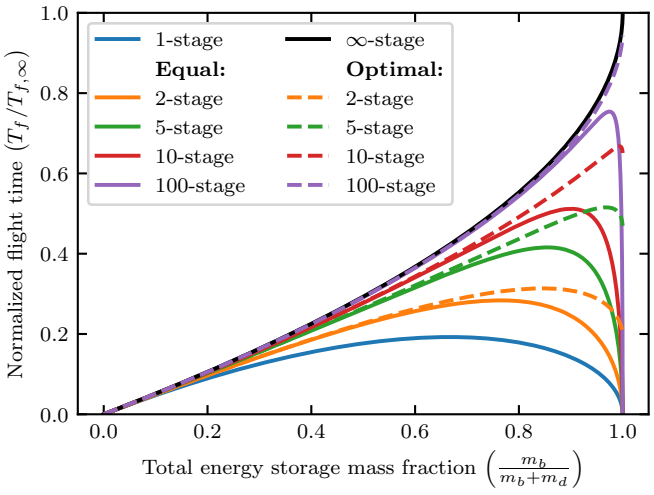

Fig. 2. Effect of total energy storage mass on hovering flight time for various number of stages. Dry mass and total energy storage mass are respectively denoted by m_d and m_b. Solid lines are for equally staged energy sources (see Section II-B.1), whereas dashed lines are for optimally staged (see Section II-B.3). The flight times are normalized with respect to that for continuously staged case with infinite energy storage mass $T_{f,\infty}$, see Eq. (25).

where we define $q\,(m) := (M+m)^{-\frac{3}{2}}$ for convenience. We note that

$$\frac{\partial}{\partial m} q\,(m) := q'\,(m) = -\frac{3}{2}\,(M+m)^{-\frac{5}{2}} < 0, \quad (10)$$

$$\frac{\partial^2}{\partial m^2} q\,(m) = \frac{15}{4}\,(M+m)^{-\frac{7}{2}} > 0, \quad (11)$$

so that we can relate the average slope of q as follows

$$\frac{q\,(m_{k+1}) - q\,(m_k)}{m_{k+1} - m_k} < q'\,(m_{k+1}) \quad (12)$$

$$< \frac{q\,(m_k + m_{k+1}) - q\,(m_{k+1})}{(m_k + m_{k+1}) - m_{k+1}}. \quad (13)$$

Rearranging this, and using $m_{k+1} > m_k > 0$ gives

$$\begin{aligned} & (m_k - m_{k+1})\, q\,(m_k + m_{k+1}) \\ & + m_{k+1} q\,(m_{k+1}) - m_k q\,(m_k) < 0. \end{aligned} \quad (14)$$

Substituting this in (9) gives $\bar{T} > T^*$. However, this contradicts the assumption that T^* is the optimal flight time, and therefore S^* cannot be an optimal staging sequence. Thus, the optimal staging sequence has $m_1 \geq m_2 \geq \ldots \geq m_N$, proceeding from the heaviest stage first to lightest stage last.

3) Optimal mass partitioning: Given a dry mass m_d, an energy storage mass budget m_b, and a total number of stages N to be used, it is of interest to find the optimal stage masses that add up to m_b, to maximize the flight time.

This is equivalent to maximizing T_f in (6) over the decision variables m_i, under the inequality constraints $m_i > 0$ and the equality constraint $\sum_i m_i = m_b$.

We define new decision variables, $x_i = m_d + \sum_{j=i}^{N} m_j$, so that $m_i = x_i - x_{i+1}$. The objective is defined as,

$$J = \sum_{i=1}^{N} \frac{x_i - x_{i+1}}{x_i^{\frac{3}{2}}}. \quad (15)$$

This can then be formulated as a constrained optimization problem as follows,

$$\max_{x_1,x_2,..,x_{N+1}} \quad J \tag{16}$$

$$\text{s.t.} \quad x_1 = m_d + m_b, \tag{17}$$

$$x_{N+1} = m_d, \tag{18}$$

$$x_{i+1} < x_i \quad \text{for} \quad i = 1, 2, \ldots, N. \tag{19}$$

Solving the above problem using the KKT conditions [20], we obtain a solution in the form of simultaneous nonlinear equations shown below,

$$\frac{1}{x_i^{\frac{3}{2}}} + \frac{2}{x_{i-1}^{\frac{3}{2}}} - \frac{3x_{i+1}}{x_i^{\frac{5}{2}}} = 0 \quad \text{for} \quad i = 2, 3, \ldots, N, \tag{20}$$

$$x_1 = m_d + m_b, \tag{21}$$

$$x_{N+1} = m_d. \tag{22}$$

Even for the simplest case of $N = 2$, this requires the roots of a fifth-degree polynomial, for which no closed-form expression exists. Nonetheless, the simultaneous equations can be solved numerically. Plots for a few sample N values are shown in Fig. 2 as dashed lines to compare with the equally staged case (solid lines). We see that for energy storage mass fraction from 0.0-0.5, there is little difference (less than 1%) between equal and optimal staging. But for fractions beyond 0.75 the difference increases to more than 5% for a small number of stages ($N = 2, 3, 4, 5$).

From the discrete staging analysis, we conclude that staging can be beneficial in the following ways. First, for the same amount of energy, we can increase the flight time as compared to a single-stage vehicle. This is to be expected because as the multi-stage vehicle ejects stages, its mass and consequently power consumption reduces. Since the total energy is the same in both cases, the flight time of the multi-stage vehicle is higher. Second, to achieve the same flight time, a multi-stage vehicle will be lighter and more compact, by a similar argument. This makes it safer and more maneuverable. Third, in the case of any multi-staged UAV, the inertia reduces with every stage ejected, thereby increasing the agility of the vehicle after each ejection.

C. Continuous staging

A vehicle powered by combustion, where the combustion products are exhausted, can be described as a limiting case of the above, with continuous staging. We consider two forms of this: using a combustion engine to provide power to rotors, and a reaction (e.g. rocket) engine.

1) Internal combustion engines: When burning (and exhausting) fuel to perform the mechanical work of driving propellers, the remaining mass of the energy storage m_E will evolve at a rate proportional to the power consumption,

$$\dot{m}_E = -\frac{1}{e_b}\dot{E} = -\frac{c_p g^{\frac{3}{2}}}{2e_b}\left(m_d + m_E\right)^{\frac{3}{2}}, \tag{23}$$

where we've used (3) and again assumed a symmetric quadcopter at hover. Solving this, and substituting $m_E\left(0\right) = m_b$, and $m_E\left(T_f\right) = 0$ gives the total flight time T_f as

$$T_f = \frac{4e_b}{c_p g^{\frac{3}{2}}\sqrt{m_d}}\left(1 - \left(1 + \frac{m_b}{m_d}\right)^{-\frac{1}{2}}\right). \tag{24}$$

This flight time value can also be derived by taking the limit as $N \to \infty$ in (7).

Note that the flight time is, as may be expected, monotonically increasing in the initial fuel mass m_b. However, there exists a natural upper limit to achievable flight time, even for arbitrarily large quantities of fuel:

$$T_f < T_{f,\infty} = \lim_{m_b \to \infty} T_f = \frac{4e_b}{c_p g^{\frac{3}{2}}\sqrt{m_d}}. \tag{25}$$

This reveals a fundamental limit of rotor propulsion. Even under the best case of continuous staging, achievable flight time has an upper limit no matter how much fuel is used. for a specific vehicle (fixed c_p), energy source (fixed e_b), fixed environment and fixed dry mass. In practice, other constraints would act to limit achievable performance, e.g. thrust and structural limitations.

We also note that as the dry mass is reduced, the flight time increases, with the limit $T_f \to \infty$ as $m_d \to 0$

2) Reaction engines: Another method of achieving continuous staging exists is reaction engines (such as rocket motors), where propellant is expelled at high velocity, producing thrust in response to the momentum flux leaving the engine. A simple analysis, assuming that fuel is expelled at a constant exhaust velocity v_e, gives a thrust force as a function of the fuel mass flow rate $\dot{m}_f$ as

$$f = \dot{m}_f v_e. \tag{26}$$

For a quadcopter-like rocket ship, with four rocket engines symmetric around the center of mass, we have that

$$4\dot{m}_f v_e = -g\left(m_d + m_f\right). \tag{27}$$

Solving this, and setting again $m_f(0) = m_b$, the achievable hover flight time is

$$T_{f,\text{rocket}} = \frac{4v_e}{g}\ln\left(1 + \frac{m_b}{m_d}\right). \tag{28}$$

This result is very closely linked to the Tsiolkovsky rocket equation [21] which describes the achievable velocity change as a function of fuel burnt, with the same functional form.

We note that this achievable flight time will grow unbounded with increasing fuel mass m_b. Thus, rocket propulsion does not suffer from the same fundamental limitation as aerodynamic propulsion. This suggests that, for certain extreme design specifications, it may be preferable to create a rocket-propelled multirotor-style robot, rather than using aerodynamic propulsion. Notable is also that, for sufficiently large gravity environments, a rocket-propelled system may again beat an aerodynamically propelled system, as g appears in the denominator with a smaller exponent.

III. Experimental Hardware Design

In this section, we explain the design of the quadcopter used in our experiments, the battery staging mechanism, and the battery switching circuit.

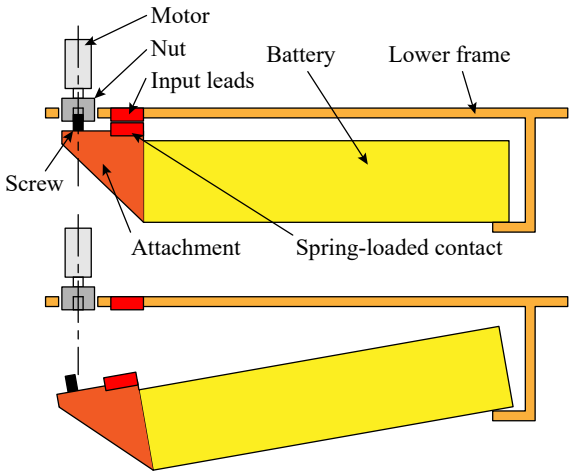

Fig. 3. Schematic of the battery-dropping mechanism

A. Vehicle design

The quadcopter is designed to have enough payload capacity for carrying useful sensors such as surveillance cameras, or environmental sensors. Its dry mass (m_d) is $565\,\mathrm{g}$, and it can generate a maximum thrust of $27\,\mathrm{N}$. Its arm length is $0.165\,\mathrm{m}$, and it uses four $0.203\,\mathrm{m}$ diameter propellers. We stack a battery switching circuit on top of the quadcopter for staging. The quadcopter is powered by two batteries, the first-stage battery placed at the bottom of the quadcopter that can be ejected when depleted, and the second-stage battery placed at the center of the quadcopter which always stays onboard. Copper plates mounted at the bottom serve as input leads from the first-stage battery. Both the first and second batteries are 3S $2.2\,\mathrm{Ah}$ lithium polymer (LiPo) batteries, weighing $190\,\mathrm{g}$ each. The staging mechanism adds an additional $30\,\mathrm{g}$ to the first battery. So the quadcopter weighs $755\,\mathrm{g}$ when carrying only the second battery, and $975\,\mathrm{g}$ when carrying both batteries. Fig. 1 shows a picture of the quadcopter.

B. Staging mechanism

The staging mechanism is shown in Fig. 3. The mechanism is placed on the lower section of the quadcopter frame. In order for the first-stage battery to engage with the mechanism, we have an attachment on one end of the battery. This attachment has a bolt, and two spring-loaded contacts, which are electrically connected to the output leads of the first-stage battery. On the side of the quadcopter frame, a "detaching" motor is installed, which has a nut fixed on its shaft. Next to the motor are two copper plates that serve as input leads from the first battery. Including all the components, the staging mechanism adds $45\,\mathrm{g}$ mass to the quadcopter.

To connect the first battery, we engage the bolt from the battery with the nut on the motor shaft. This connects the spring-loaded contacts to the input leads. To disconnect the battery, we command the motor to unscrew the bolt. When the bolt is completely disengaged from the nut, the battery loses support and thus drops.

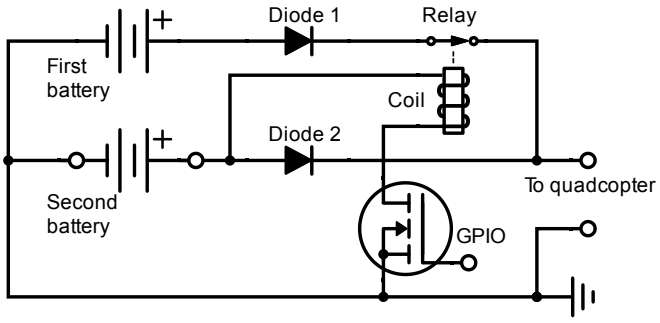

Fig. 4. Schematic of the battery switching circuit.

C. Battery switching circuit

The design of our battery switching circuit is inspired by [9]. Since our system is flying, we cannot afford to cut the power supply when switching from the first battery to the second battery. The two batteries need to be connected in parallel for some time to achieve this. We connect diodes in series with each of the batteries to avoid reverse currents due to the voltage difference between the batteries.

A normally closed relay is connected in series with the first battery. By opening the switch, we can draw power from the first battery even when it is at a lower voltage than the second battery. This is necessary to completely consume the first battery, before starting the use of the second battery. The relay coil is connected across the first battery input leads in series with a MOSFET. The gate terminal of the MOSFET is connected to a GPIO pin on the flight controller to control the relay. Fig. 4 shows a schematic diagram of the battery switching circuit. The circuit weighs $60\,\mathrm{g}$.

IV. Experimental Validation

We validate the staging analysis by first predicting the flight times for our quadcopter with and without staging. We then conducting hovering flight experiments for single-stage and two-stage cases. The flight times in the two cases are compared to each other to show that flight time for the multi-stage case is higher. The experimental flight times are also compared with the predictions from the analysis and are shown to match well, validating the analysis.

A. Flight time prediction from analysis

We use the results from equal staging (Section II-B.1) since we use the same battery for both stages. From the datasheet of the batteries that we use, the specific energy value is $e_b = 130\,\mathrm{Wh\,kg^{-1}}$. The value of c_T is determined empirically from flight experiments on the quadcopter, which is $c_T = 6.2 \times 10^{-3}\,\mathrm{kg^{\frac{3}{2}}\,W^{-1}}$. Using Eq. (7) with $m_d = 0.565\,\mathrm{kg}$ as dry mass and $m_b = 0.380\,\mathrm{kg}$ as total battery mass, we predict flight times of $19.69\,\mathrm{min}$ for the single-stage case, and $23.58\,\mathrm{min}$ for the two-stage case.

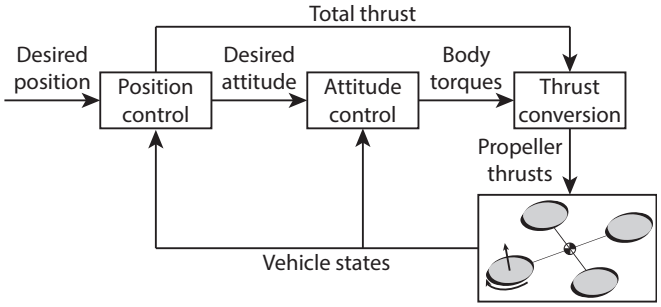

Fig. 5. Block diagram of the quadcopter controller.

B. Experimental setup

The quadcopter used in our experiments is localized via sensor fusion of a motion capture system and an onboard rate gyroscope [22]. Experimental data from the motion capture system, voltage sensor, and the current sensor is logged via radio for post-processing. We control the quadcopter using a cascaded position and attitude controller shown in Fig. 5.

C. Demonstration

The benefit of staging batteries is demonstrated by conducting two types of experiments: one without staging (single-stage), and the other with staging (two stages). The flight experiments can be seen in the video attachment.

In the single-stage experiments, the quadcopter hovers using the two batteries until both the batteries are completely discharged. A battery is considered completely discharged when it reaches $3.0\,\mathrm{V}$ per cell. We do two experiments in this category:

1) Both batteries are consumed simultaneously.
2) First and second batteries are consumed successively.

The quadcopter hovered for $19.7\,\mathrm{min}$ with simultaneous consumption, and $19.3\,\mathrm{min}$ with successive consumption.

In the two-stage experiment, the quadcopter initially hovers using the first battery. Once the first battery is discharged, the second battery is connected to the quadcopter by closing the relay in the switching circuit. The first stage is then detached by activating the detaching motor in the staging mechanism. Hovering continues until we completely consume the second battery. Fig. 7 shows a sequence of snapshots from the two-stage experiment. The quadcopter hovered for a total of $23.6\,\mathrm{min}$ in this experiment.

D. Discussion

The plots of input voltage and power vs. time for the experiments are shown in Fig. 6. We see the characteristic LiPo battery discharge curve [23] in each of the voltage vs. time plots.

We compare the single-stage successive consumption experiment with the two-stage experiment. The first discharge curve shows the complete consumption of the first battery, and the next one shows the complete consumption of the second battery. Since the quadcopter has the same total mass in both experiments when consuming the first battery, we

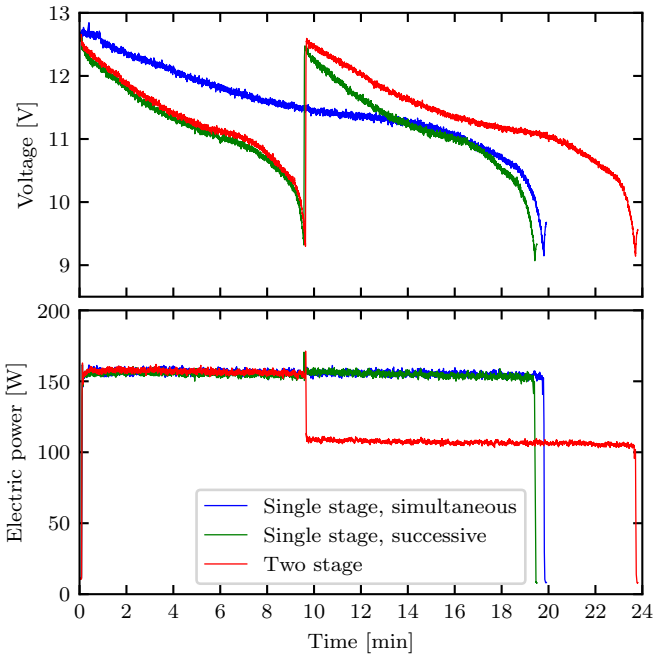

Fig. 6. Input voltage and power vs. time for the quadcopter. Values are measured at the output of the battery.

expect that this discharge would take approximately the same time in both cases. The voltage vs. time plot shows that this is indeed the case. However, during the consumption of the second battery, the quadcopter has different masses in the two experiments. In the two-stage experiment where we detach the first battery, the quadcopter mass is lower. We expect the power consumption to be lower and consequently the flight time to be higher for this case. The voltage and power vs. time plot confirms that this is true.

The power vs. time plot shows that power input to the quadcopter remains approximately constant to hover continuously, as long as its mass is not changing. For the single-stage experiments, we see that this is true for the entire duration of the experiment. For the two-stage experiment, we see that the power input remains constant until the first battery is completely discharged. Once we detach the first stage, the power consumption settles to a lower value needed to hover at the reduced mass.

An important observation here is energy consumption (calculated from the power vs. time plot) is approximately the same for all experiments. This is to be expected since we have the same total energy in all cases. The energy consumption in the three experiments (single-stage simultaneous, single-stage successive, and two-stage) respectively are $1.848 \times 10^5\,\mathrm{J}$, $1.800 \times 10^5\,\mathrm{J}$, and $1.805 \times 10^5\,\mathrm{J}$. We note that the values mentioned here are the output energy utilized by the quadcopter. In the single-stage successive consumption experiment and two-stage experiment, since we are using one battery at a time, the effective internal resistance is the same, which results in similar electrical efficiency. In the single-stage simultaneous consumption experiment

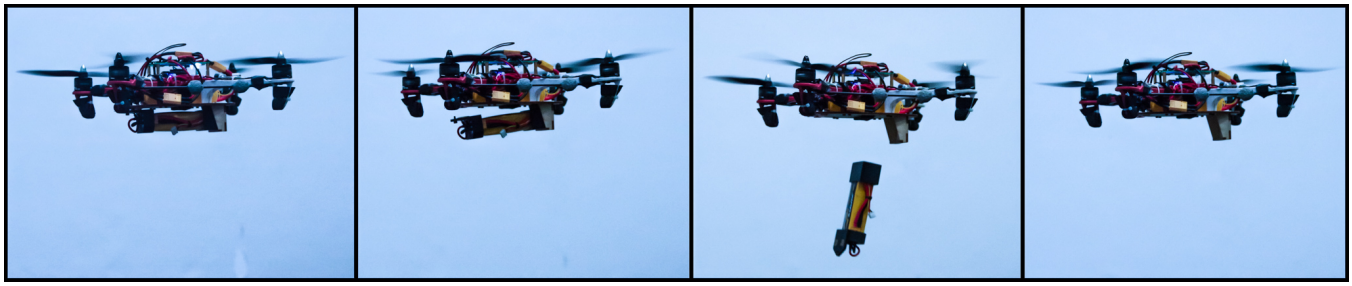

Fig. 7. Sequence of images from the two-stage flight experiment. From left to right: (a) Quadcopter hovers using only first battery. (b) First battery is depleted. Quadcopter starts using second battery. The detaching motor is simultaneously activated to disengage the bolt. First stage is about to fall. (c) First stage is ejected and freely falls towards the ground. (d) Quadcopter continues hovering using the second battery, and its mass and power consumption is reduced. **Note:** We have not attached a parachute in this case to clearly show how the staging works. The first stage fall is broken softly by a net below the quadcopter. In real-life settings, especially outdoors, it is advised to use some fall breaking mechanism to not damage the energy source or any property.

however, we are using two batteries in parallel which, in essence, halves the internal resistance. This increases the electrical efficiency, and thus the quadcopter is able to utilize more output energy for the same input energy. Consequently, we get a slightly higher flight time as compared to the single-stage successive consumption experiment. To be fair in comparing staged and unstaged cases, we use the higher flight time ($19.7\,\mathrm{min}$) for the single-stage case.

We see that the flight time predictions match well with the experimental values, with less than 2% difference. Part of the reason for this accuracy is the empirical determination of the parameters. However, it does validate that the assumptions used in the staging analysis are, in fact, realistic.

In addition, we compute the battery mass required for a single-stage vehicle to give us the same flight time as is obtained with two stages. Using Eq. (7) with $T_f = 23.6\,\mathrm{min}$, $m_d = 565\,\mathrm{g}$, $N = 1$, and e_b and c_T same as before, we calculate $m_b = 635\,\mathrm{g}$. So a single-stage vehicle would need an additional $255\,\mathrm{g}$ of battery to achieve the same flight time as a two-stage vehicle. Even considering the additional mass added by the staging mechanism and the switching circuit, we save $150\,\mathrm{g}$ or about 26% of the dry mass by using just one additional stage.

We list a few shortcomings of staging energy sources to wrap this section up. First, since we are ejecting energy sources in-flight which are potentially hazardous, care needs to be taken to land them safely to avoid polluting the environment, and to avoid any damage to the energy source or its surroundings. Secondly, these energy sources are reusable and it would be a waste to simply discard the ejected stages. So careful planning is necessary for the recovery of these ejected stages. Lastly, we see that adding a stage requires the design of a mechanism to eject that stage, which adds to the mass and complexity of the quadcopter. Although the ejection mechanism does involve detailed design, we saw in the last paragraph that the additional mass of the mechanism plus the circuit is well compensated by the flight time and mass benefits of staging.

V. Conclusion and Future Work

A. Conclusion

In this paper, we have introduced the concept of staging energy sources for UAVs, specifically considering multirotors for our analysis. The idea is to discard the energy sources that cannot supply power anymore. This reduces the mass of the vehicle, thereby reducing power consumption. This, in turn, increases the overall flight time of the vehicle.

We presented a model to predict the flight time of a multi-stage multirotor with given physical parameters related to the energy source and power consumption. We then analyzed two specific cases of optimal staging. First, given N energy storage stages of fixed, known masses, we proved that flight time can be maximized by staging them in order of decreasing mass, with the heaviest stage being depleted and ejected first. Second, given an energy storage mass budget, finding the optimal way of partitioning it into N stages to maximize the flight time. This problem does not have a closed-form solution. Numerical results were presented and compared with the equal staging case. From the discrete staging analysis, we conclude that the choice of number of stages matters more than optimally partitioning the stages.

We also presented an analysis for continuous staging for two cases: internal combustion engines driving propellers, and reaction engines. We observed that there is a fundamental limit on flight time when using I.C. engines, even when using an unlimited amount of fuel, which does not exist for reaction engines. We also noticed that the dependence on gravity was different for the two engines. So in particular cases, e.g. higher gravity environments (other planets or moons), reaction engines could be a preferred choice over aerodynamic propulsion for longer flight times.

We designed a two-stage quadcopter with a staging mechanism to detach a used battery in-flight, and conducted hovering flight experiments for two cases: single-stage and two-stage. Flight times were predicted from the analysis for the single-stage and two-stage case, with the two-stage case showing a 20% higher flight time for the same battery mass. Experimental flight times matched the predictions well (within 2%) with observed flight times of $19.7\,\mathrm{min}$ for the

single-stage case and $23.6\,\mathrm{min}$ for the two-stage case. This validates the staging analysis

We note that the potential gains of using more stages are even higher, with certain flight times not achievable by a single-stage vehicle. Since higher flight times can be achieved via staging without adding as much battery mass as required for a single stage, usually none or minimal changes to the vehicle's structure and powertrain would be required. Moreover, the inertia of the vehicle reduces with every battery ejected, thereby increasing its agility after each ejection.

B. Limitations

Limitations of the staging approach include the requirement of careful ejection, landing, and recovery of the energy source, and intricate design of the staging mechanism. This is to minimize damage to the energy source as well as its surroundings. We saw that the shortcomings were compensated by the flight time benefit by comparing masses of single-stage and two-stage vehicles that have similar flight times.

C. Extensions

Future work may include the use of additional stages to further increase in flight time, or to decrease mass for the same flight time as the lower stage versions. This would entail a more intricate design for ejection of each stage individually and seamless switching between the usage of these energy sources. Another extension could be exploring the design and control of a multirotor using reaction engines as thrusters. This would require careful design to have actuation in the desired degrees of freedom. A third extension could be the planning of locations for stage ejections in an urban setting, so that collection of these ejected stages can be localized and potentially automated.

ACKNOWLEDGMENT

We gratefully acknowledge financial support from NAVER LABS and Code42 Air.

The experimental testbed at the HiPeRLab is the result of contributions of many people, a full list of which can be found at `hiperlab.berkeley.edu/members/`.

REFERENCES

[1] A. Jaimes, S. Kota, and J. Gomez, "An approach to surveillance an area using swarm of fixed wing and quad-rotor unmanned aerial vehicles uav (s)," in *2008 IEEE International Conference on System of Systems Engineering*. IEEE, 2008, pp. 1–6.

[2] S. Siebert and J. Teizer, "Mobile 3d mapping for surveying earthwork projects using an unmanned aerial vehicle (uav) system," *Automation in construction*, vol. 41, pp. 1–14, 2014.

[3] C. A. Thiels, J. M. Aho, S. P. Zietlow, and D. H. Jenkins, "Use of unmanned aerial vehicles for medical product transport," *Air medical journal*, vol. 34, no. 2, pp. 104–108, 2015.

[4] M. Erdelj, E. Natalizio, K. R. Chowdhury, and I. F. Akyildiz, "Help from the sky: Leveraging uavs for disaster management," *IEEE Pervasive Computing*, vol. 16, no. 1, pp. 24–32, 2017.

[5] D. Lee, J. Zhou, and W. T. Lin, "Autonomous battery swapping system for quadcopter," in *2015 International Conference on Unmanned Aircraft Systems (ICUAS)*. IEEE, 2015, pp. 118–124.

[6] T. Toksoz, J. Redding, M. Michini, B. Michini, J. P. How, M. Vavrina, and J. Vian, "Automated battery swap and recharge to enable persistent uav missions," in *AIAA Infotech@ Aerospace Conference*, vol. 21, 2011.

[7] N. K. Ure, G. Chowdhary, T. Toksoz, J. P. How, M. A. Vavrina, and J. Vian, "An automated battery management system to enable persistent missions with multiple aerial vehicles," *IEEE/ASME transactions on mechatronics*, vol. 20, no. 1, pp. 275–286, 2014.

[8] E. Barrett, M. Reiling, S. Mirhassani, R. Meijering, J. Jager, N. Mimmo, F. Callegati, L. Marconi, R. Carloni, and S. Stramigioli, "Autonomous battery exchange of uavs with a mobile ground base," in *2018 IEEE International Conference on Robotics and Automation (ICRA)*. IEEE, 2018, pp. 699–705.

[9] K. P. Jain and M. W. Mueller, "Flying batteries: In-flight battery switching to increase multirotor flight time," *arXiv preprint arXiv:1909.10091*, 2019.

[10] H.-P. Thamm, N. Brieger, K. Neitzke, M. Meyer, R. Jansen, and M. Mönninghof, "Songbird-an innovative uas combining the advantages of fixed wing and multi rotor uas." *International Archives of the Photogrammetry, Remote Sensing & Spatial Information Sciences*, vol. 40, 2015.

[11] A. S. Saeed, A. B. Younes, C. Cai, and G. Cai, "A survey of hybrid unmanned aerial vehicles," *Progress in Aerospace Sciences*, vol. 98, pp. 91–105, 2018.

[12] C. Holda, B. Ghalamchi, and M. W. Mueller, "Tilting multicopter rotors for increased power efficiency and yaw authority," in *2018 International Conference on Unmanned Aircraft Systems (ICUAS)*. IEEE, 2018, pp. 143–148.

[13] A. Tagliabue, X. Wu, and M. W. Mueller, "Model-free online motion adaptation for optimal range and endurance of multicopters," in *2019 International Conference on Robotics and Automation (ICRA)*. IEEE, 2019, pp. 5650–5656.

[14] K. C. Reinhardt, T. R. Lamp, J. W. Geis, and A. J. Colozza, "Solar-powered unmanned aerial vehicles," in *IECEC 96. Proceedings of the 31st Intersociety Energy Conversion Engineering Conference*, vol. 1. IEEE, 1996, pp. 41–46.

[15] A. Johanning, M. Pagitz, and J. M. Mirats-Tur, "Celldrone - a modular multi-rotor aircraft," in *Deutscher Luftund Raumfahrtkongress*, 2011.

[16] H. Hall and E. Zambelli, "On the optimization of multistage rockets," *Journal of Jet Propulsion*, vol. 28, no. 7, pp. 463–465, 1958.

[17] R. D. Geckler, "Ideal performance of multistage rockets," *ARS Journal*, vol. 30, no. 6, pp. 531–536, 1960.

[18] J. Gray and R. Alexander, "Cost and weight optimization for multistage rockets," *Journal of Spacecraft and Rockets*, vol. 2, no. 1, pp. 80–86, 1965.

[19] B. W. McCormick, "Aerodynamics aeronautics and flight mechanics," 1995.

[20] S. Boyd and L. Vandenberghe, *Convex optimization*. Cambridge university press, 2004.

[21] M. J. Turner, *Rocket and spacecraft propulsion: principles, practice and new developments*. Springer Science & Business Media, 2008.

[22] K. P. Jain, T. Fortmuller, J. Byun, S. A. Mäkiharju, and M. W. Mueller, "Modeling of aerodynamic disturbances for proximity flight of multirotors," in *2019 International Conference on Unmanned Aircraft Systems (ICUAS)*. IEEE, 2019, pp. 1261–1269.

[23] N. Navarathinam, R. Lee, and H. Chesser, "Characterization of lithium-polymer batteries for cubesat applications," *Acta Astronautica*, vol. 68, no. 11-12, pp. 1752–1760, 2011.